frontiers | Frontiers in Earth Science

ORIGINAL RESEARCH
published: 28 June 2022
doi: 10.3389/feart.2022.929777

Experimental Study on the Evolution of Dynamic Pore Pressure and Unidirectional and Bidirectional Vibrations of Phosphogypsum

Fuqi Kang[1,2], *Guangjin Wang*[1,2]*, *Wenlian Liu*[3], *Kui Zhao*[4], *Menglai Wang*[5], *Xiaoshuang Li*[6], *Wen Zhong*[4] *and Zhicheng Dong*[1]

[1]Faculty of Land Resources Engineering, Kunming University of Science and Technology, Kunming, China, [2]Yunnan International Technology Transfer Center for Mineral Resources Development and Solid Waste Resource Utilization, Kunming, China, [3]China Nonferrous Metals Industry Kunming Survey and Design Research Institute Co. LTD., Kunming, China, [4]School of Resources and Environmental Engineering, Jiangxi University of Science and Technology, Ganzhou, China, [5]National Engineering Research Center for Development and Utilization of Phosphorus Resources, Yunnan Phosphate Group Co. LTD., Kunming, China, [6]School of Civil Engineering, Shaoxing University, Shaoxing, China

Under seismic action, the stock of phosphogypsum (PG) affects the security risk significantly, so it is crucial to study the dynamic characteristics of PG. In this article, unidirectional and bidirectional vibration tests on typical PG in Yunnan under different consolidation-confining pressure and vibration conditions were carried out using a dynamic triaxial apparatus that can be used for bidirectional vibration. The results show that the pore pressure growth of PG under both unidirectional and bidirectional vibrations has obvious stages and can be fitted by the BiDoseResp function. The dynamic strength of PG does not increase monotonically with the increase in consolidation-confining pressure and dynamic stress under the same cyclic stress ratio (CSR) but varies under a specific critical condition. The dynamic strength of PG decreases significantly with the increase in CSR under unidirectional and bidirectional vibrations. The number of vibrations required for liquefaction by bidirectional vibrations is much larger than that by unidirectional vibrations under the same CSR conditions, and the specimens have significant softening characteristics after liquefaction by bidirectional vibrations. The study results can provide theoretical references for studying the dynamic stability of PG reservoirs under seismic action.

Keywords: phosphogypsum, dynamic triaxial test, bidirectional vibration, cyclic stress ratio, dynamic pore pressure, softening

OPEN ACCESS

Edited by:
Min Wang,
Los Alamos National Laboratory (DOE), United States

Reviewed by:
Tiande Wen,
Shantou University, China
Xiangcou Zheng,
Delft University of Technology, Netherlands

***Correspondence:**
Guangjin Wang
wangguangjin2005@163.com

Specialty section:
This article was submitted to Geohazards and Georisks, a section of the journal Frontiers in Earth Science

Received: *27 April 2022*
Accepted: *18 May 2022*
Published: *28 June 2022*

Citation:
Kang F, Wang G, Liu W, Zhao K, Wang M, Li X, Zhong W and Dong Z (2022) Experimental Study on the Evolution of Dynamic Pore Pressure and Unidirectional and Bidirectional Vibrations of Phosphogypsum. Front. Earth Sci. 10:929777. doi: 10.3389/feart.2022.929777

1 INTRODUCTION

Phosphogypsum (PG) is a by-product of the production process of wet phosphoric acid. In recent years, the market demand for phosphorus compound fertilizer has been increasing, and the emission of PG has also been increasing (Cao et al., 2021). However, the utilization rate of PG is less than 40%, a large number of unused PG piles on the ground form PG dams, and the worldwide stockpile has reached six billion tons (Zhang et al., 2019). Phosphogypsum ponds are necessary production facilities for phosphate mines and phosphorus chemical industries and are also one of the major sources of danger. Wet PG ponds are tailings ponds. Among the various factors leading to tailings

pond accidents, earthquakes are the second most important factor after heavy rainfall (Rico et al., 2008). Some of the PG ponds in operation in China are located in high-intensity seismic regions (Mi et al., 2015). Once the dams are destabilized, they will have catastrophic consequences for the downstream areas of the dams (Wang et al., 2021; Zheng et al., 2022). The former State Administration of Work Safety of China (now merged into the Ministry of Emergency Management of the People's Republic of China, 2016) issued *Safety technical regulation on phosphogypsum stack (AQ 2059-2016)*, and explicitly stipulated that the design of PG ponds must meet the dynamic stability requirements.

The current research on PG mainly focuses on comprehensive utilization, and there is little research on the physical and mechanical properties and other aspects of PG. Xu et al. (2008) found that PG had strong shear strength and good water stability. Shen et al. (2008) found that PG had a plate-like crystal structure, a liquid-plastic limit similar to that of powdered soil, good permeability, and unique compression and consolidation characteristics. Tayibi et al. (2009) found that the solubility of PG had a strong relationship with PH value and found that most of the particles had rhombic or monoclinic crystal structures using scanning electron microscopy. Zhang et al. (2007) studied the relationship between the solubility of PG and temperature and found that PG had obvious shear expansion characteristics in a consolidated undrained test. Mi et al. (2015) found that deposited PG had obvious anisotropy, a high friction angle, and anti-liquefaction ability. Lu et al. (2021) divided the stress-strain curve of typical PG in a triaxial shear test into three stages and summarized the dynamic parameters, such as dynamic strength, dynamic shear modulus, and damping ratio of PG, and their variation laws by a dynamic triaxial test.

Many scholars have studied the dynamic properties of rock and soil under cyclic action and achieved a lot of results (You et al., 2021; Zhou et al., 2022). Seed et al. (1966) proposed to express the relationship between the pore pressure ratio and the loading period ratio by the inverse sine trigonometric function through a dynamic triaxial test of saturated sandy soil, providing a theoretical basis for the subsequent research on the development law of the dynamic pore pressure of soil. Zhang et al. (2006) modified the Seed pore pressure model and proposed the dynamic pore pressure prediction formula applicable to tailing materials. Wang et al. (2012) conducted dynamic triaxial tests on lime-treated expansive soil with different confining pressures, vibration frequencies, consolidation ratios, and cycle numbers to discuss the dynamic properties of lime-treated expansive soil. Du et al. (2016) studied the pore pressure growth characteristics of tailing soils under cyclic loading, proposed their pore pressure growth model, and pointed out that the model was also applicable to sandy soils. Zhang et al. (2018) studied the evolution law of dynamic pore pressure of tailings under different consolidation conditions, indicated the obvious stages in the evolution of dynamic pore pressure of tailings, and deduced the critical pore water pressure equations under isostatic consolidation and anisotropic consolidation based on the limit equilibrium theory.

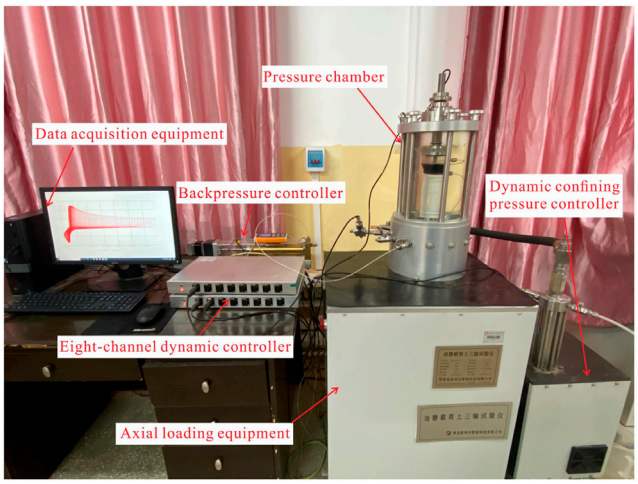

FIGURE 1 | KTL-DYN10 bidirectional dynamic triaxial apparatus.

In the previous analyses of seismic responses, the seismic action was considered to be dominated by horizontal shear, so the unidirectional vibration cyclic load was used to simulate the seismic motion (Seed et al., 1971). In the near-field seismic action, the effect of vertical seismic force is not negligible, so using bidirectional vibrations to simulate the seismic action is more practical. In recent years, many scholars have studied the dynamic properties of soil under bidirectional vibrations. Rascol (2009) studied the coupled stress paths of dynamic spherical stress and dynamic partial stress with bidirectional vibrations under undrained conditions of saturated sandy soil. They found that the dynamic pore pressure and dynamic modulus of soil change with the amplitude of dynamic spherical stress and phase difference. Idriss et al. (1978) proposed the softening index and established the expression between the softening index and the number of cycles. Wang et al. (2009) found that the increase in cyclic partial stress and radial cyclic stress could accelerate the softening of soil when the saturated soft clay soil was under bidirectional vibrations. Xie et al. (2017) conducted multiple sets of unidirectional and bidirectional vibration tests on saturated clay and found that the accumulated plastic strain of specimens developed faster under unidirectional vibrations at the same stress level. Liu et al. (2021) found obvious phases in developing the accumulated pore pressure of saturated tailing sand under high-stress conditions and preliminarily established the dynamic pore pressure growth model of tailing silt under unidirectional and bidirectional vibrations.

Due to the limitation of test apparatuses and other reasons, there are few reports on the research of dynamic characteristics of PG under unidirectional and bidirectional vibrations. In this article, the KTL-DYN10 bidirectional dynamic triaxial apparatus (Qiankunxing Intelligent Technology Company, Qingdao, China) was used to conduct dynamic triaxial tests on PG under different consolidation and vibration conditions to explore the dynamic strength change law and damage mechanism of PG under different cyclic vibration

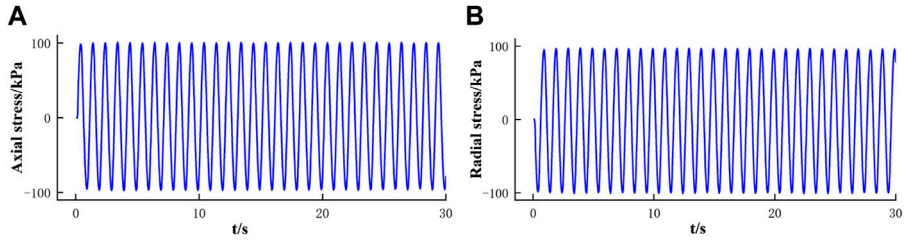

FIGURE 2 | Time–history curves measured under bidirectional vibrations: **(A)** Time–history curves of axial stress; **(B)** time–history curves of radial stress.

TABLE 1 | Chemical components of PG/%.

Al_2O_3	CaO	SO_3	H_2O (crystal water)	MgO	P_2O_5	Fe_2O_3
0.91	30.46	43.83	19.46	0.39	0.75	0.21

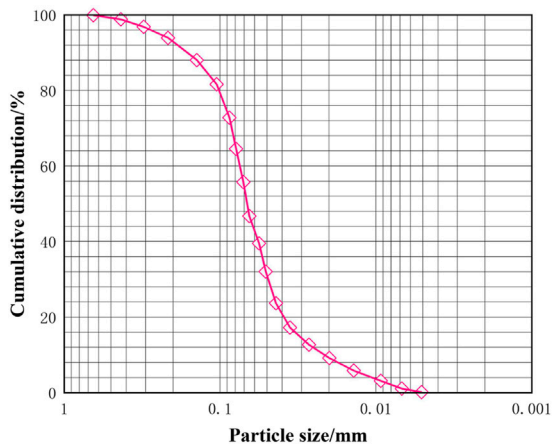

FIGURE 3 | Cumulative curve of the particle size distribution of PG.

FIGURE 4 | Test sample.

conditions and provide a design basis for the seismic stability of PG dams.

2 EXPERIMENTAL CONTENT AND METHODS

2.1 Test Equipment

In the test, KTL-DYN10 bidirectional dynamic triaxial apparatus was applied, as shown in **Figure 1**. The hardware system includes axial loading equipment, a dynamic confining pressure controller, a backpressure controller, a pressure chamber, an eight-channel dynamic controller, and data acquisition equipment. The software system is a DSP high-speed digital control system with a maximum operating frequency of up to 50 Hz and a maximum dynamic stress amplitude of up to ±10 kN. **Figure 2** shows the time-history curves of axial and radial loads measured simultaneously when the dynamic load is 100 kPa. It can be seen from the figure that the axial and radial loads are stable, indicating that the apparatus has good performance and the test results are credible.

2.2 Test Soil Sample and Test Preparation

The PG used in this experiment was taken from a PG pond discharged from a group in Yunnan after producing phosphoric acid. The PG is dark gray. Its chemical components are shown in **Table 1**, and its main component is gypsum dihydrate. The measuring results of the test show that the liquid limit of PG is 26.8%, the plastic limit is 18.4%, and the plasticity index is 8.4. The diameters of its particles are mainly between 0.005 and 0.075 mm, closer to that of pulverized soil, and the cumulative curve is shown in **Figure 3**. The inhomogeneity coefficient Cu is 3.45, and the curvature coefficient Cc is 1.52. The above analyses show that the PG has a concentrated particle size, a narrow distribution range, and good uniformity, which is not conducive to the stability of the tailings ponds.

TABLE 2 | Test scheme.

Test number	Consolidation confining pressure σ_0'/kPa	Dynamic stress σ_d/kPa	CSR	Cycle termination weeks/N	Vibration mode
1-1	100	50	0.25	725	Unidirectional vibration
1-2	150	75		538	
1-3	200	100		270	
1-4	250	125		373	
1-5	300	150		457	
1-6	600	300		1,070	
2-1	200	60	0.15	458	Unidirectional vibration
2-2		100	0.25	271	
2-3		140	0.35	152	
2-4		180	0.45	36	
3-1	200	30	0.15	3,450	Bidirectional vibration
3-2		50	0.25	2,540	
3-3		70	0.35	2009	
3-4		90	0.45	1,220	

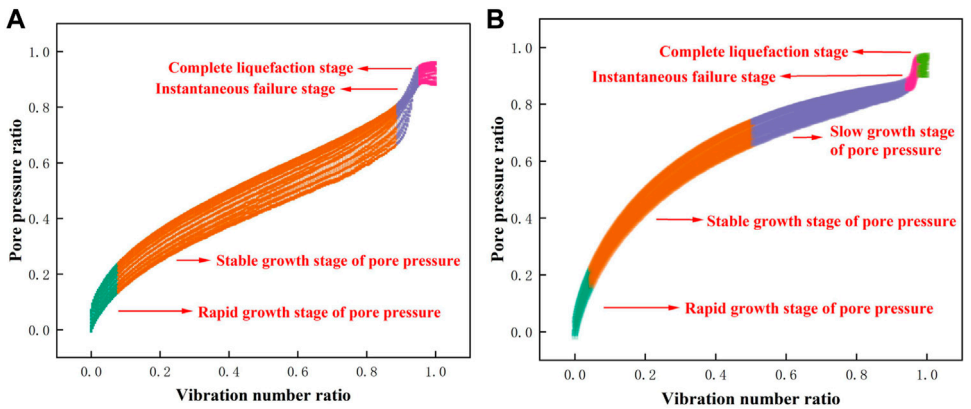

FIGURE 5 | Development curves of instantaneous pore pressure of typical PG: **(A)** unidirectional vibrations; **(B)** bidirectional vibrations.

The main component of PG is gypsum dihydrate. When the temperature exceeds 60°C, dihydrate gypsum starts to dehydrate and becomes hemihydrate gypsum or anhydrous gypsum, as shown in **Eq. 1**:

$$CaSO_4 \cdot 2H_2O \rightarrow CaSO_4 \cdot 0.5H_2O \rightarrow CaSO_4 \ (\textbf{thermal dehydration}) \quad (1)$$

Therefore, in the process of specimen preparation, to avoid losing crystal water during drying, according to the China national standard *Phosphogypsum* (Global, 2018), the drying temperature of PG is suggested to be 40 ± 2°C. In the test, cylindrical specimens with a diameter of 50 mm and a height of 105 mm that were compacted in four layers were used, as shown in **Figure 4**. According to the deposition law in most PG dams, the dry densities of the samples were determined to be 1.12 g/cm^3.

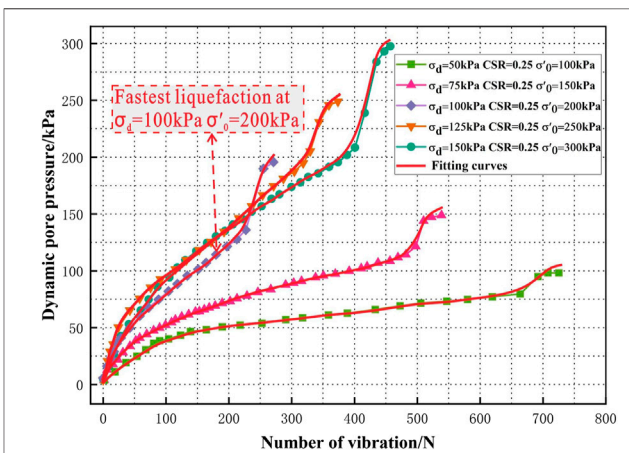

FIGURE 6 | Development curves of accumulated pore pressure under unidirectional vibrations with the same CSR conditions.

2.3 Test Scheme

Under unidirectional vibrations, $CSR = \sigma_d/2\sigma_0'$. Under bidirectional vibrations, $CSR = \sigma_d/\sigma_0'$. Under the same CSR conditions, cyclic dynamic stress of σ_d was applied in the axial direction under unidirectional vibrations, and cyclic dynamic stress of $\sigma_d/2$ was applied in the radial and axial directions under bidirectional vibrations. A sine wave was chosen for the test, the vibration frequency was 1 Hz, and the phase angle was set to **180°** for bidirectional vibrations. The pore pressure reaching 95% of the consolidation confining pressure during the liquefaction was used as the damage standard of PG. After the specimens were prepared, they were saturated with CO_2, distilled water, and back pressure to increase the saturation of the specimens. When the saturation reached 97% (B > 0.97), the consolidation was carried out under the corresponding conditions, and the dynamic load was applied after the consolidation was completed.

Fourteen sets of valid test data were obtained. Six groups of tests were designed under the same CSR conditions with unidirectional vibrations, and the consolidation-confining pressure and dynamic stress were gradually increased. The other eight groups of tests were performed under the same consolidation confining pressure, and the CSR was continuously increased under unidirectional and bidirectional vibrations. The specific test scheme is shown in **Table 2**.

3 TEST RESULTS AND ANALYSIS

3.1 Pore Pressure Growth Characteristics of PG Under Unidirectional and Bidirectional Vibrations

Under seismic action, PG dams have the risk of liquefaction and instability. Their evolution law of pore pressure can reflect their liquefaction process. Therefore, it is necessary to analyze the development law of pore pressure when studying the dynamic characteristics of PG under unidirectional and bidirectional vibrations.

The thickness of the development curves of instantaneous pore pressure indicates the difference between the maximum and minimum pore pressure in this vibration cycle, which is related to the dynamic strength of the specimens and the applied dynamic stress. **Figure 5** shows the growth curves of instantaneous pore pressure of typical PG under unidirectional and bidirectional vibrations, vibration number ratio is the ratio of current vibration times to pore pressure corresponding to liquefaction, and pore pressure ratio is the ratio of current pore pressure to consolidation confining pressure. Under the same conditions, cyclic dynamic stress of $\boldsymbol{\sigma_d}$ was applied in the axial direction under unidirectional vibrations, and cyclic dynamic stress of $\boldsymbol{\sigma_d/2}$ was applied in the radial and axial directions under bidirectional vibrations. The axial and radial dynamic stresses are equal in size and opposite in direction, and the phase angle is 180°. So the dynamic stress applied under unidirectional vibrations is two times that under bidirectional vibrations, and the thickness of the curves of the instantaneous pore pressure under unidirectional vibrations is significantly greater than that under bidirectional vibrations.

According to the growth curve of instantaneous pore pressure and the range of pore pressure ratio, under unidirectional vibrations, the liquefaction process of PG can be divided into four stages (**Figure 5A**): the rapid growth stage of pore pressure (pore pressure ratio between 0 and 0.2), the stable growth stage of pore pressure (pore pressure ratio between 0.2 and 0.7), the instantaneous failure stage (pore pressure ratio between 0.7 and 0.9), and the complete liquefaction stage (pore pressure ratio between 0.9 and 1.0). Under bidirectional vibrations, the liquefaction process can be divided into five stages (**Figure 5B**): the rapid growth stage of pore pressure (pore pressure ratio between 0 and 0.2), the stable growth stage of pore pressure (pore pressure ratio between 0.2 and 0.7), the slow growth stage of pore pressure (pore pressure ratio between 0.7 and 0.85), the instantaneous failure stage (pore pressure ratio between 0.85 and 0.9), and the complete liquefaction stage (pore pressure ratio between 0.9 and 1.0).

At the rapid growth stage of pore pressure, the pore pressure increases rapidly, and the growth curve is convex. At the stable growth stage of pore pressure, the pore pressure increases steadily, the growth curve of instantaneous pore pressure is thick, and the PG has a high anti-liquefaction ability. The slow growth stage of pore pressure exists only under bidirectional vibrations, the growth rate of pore pressure gradually decreases at this stage, and the specimens maintain high strength. At the instantaneous failure stage, the pore pressure increases sharply, the difference between the maximum and minimum pore pressure decreases rapidly, the PG structure is destroyed rapidly, and the liquefaction strength is significantly reduced. At the complete liquefaction stage, the pore pressure approaches consolidation confining pressure; the growth rate of pore pressure is significantly reduced; the specimens are completely liquefied; the internal structure of PG is completely destroyed; the particles move disorderly; a large amount of interparticle pore water and bound water discharge continuously, so the curves of instantaneous pore pressure thicken again.

3.2 The Development Law of Pore Pressure and Analysis of the Dynamic Stress-Strain Curves of PG Under the Same CSR Conditions

3.2.1 The Development Law of the Pore Pressure of PG Under the Same CSR Conditions

According to the general law of soil dynamics (Xie et al., 2011), higher consolidation confining pressure indicates greater corresponding burial depth, tighter interparticle connection, and stronger anti-liquefaction ability. With the increase in dynamic stress, the seismic ability increases, while the anti-liquefaction ability decreases. However, the effect of the simultaneous action of the consolidation confining pressure and the dynamic stress on the dynamic properties of PG is unclear, so this section explores the joint effect of simultaneously increasing the two on the dynamic strength

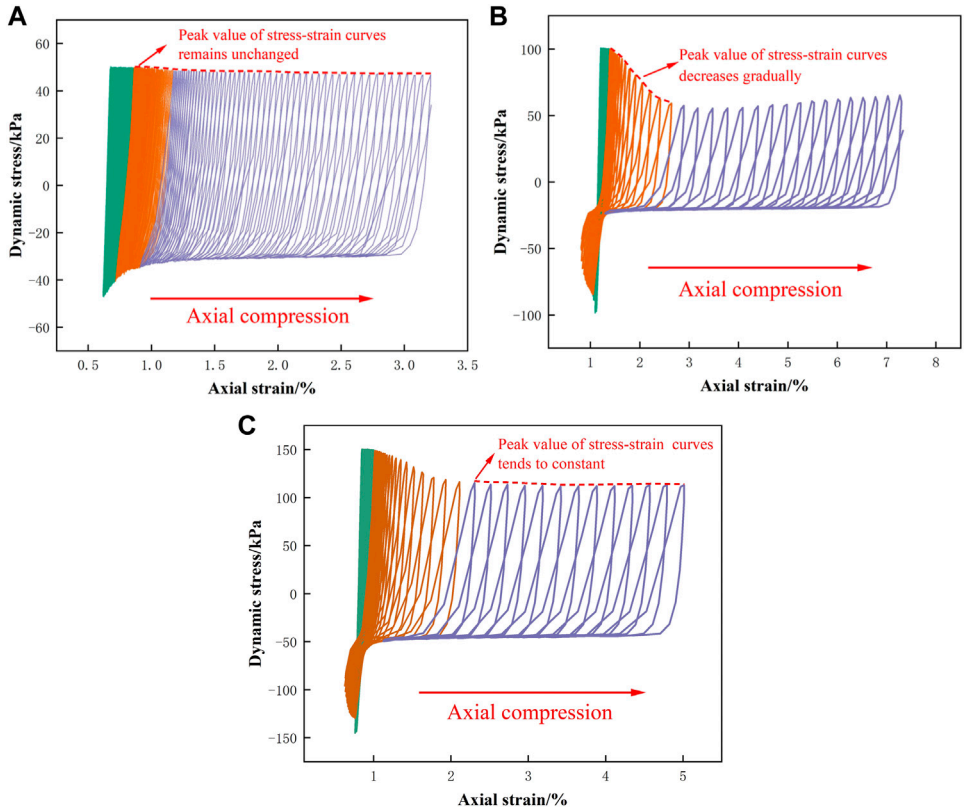

FIGURE 7 | Dynamic stress–strain curves under different stress conditions with the same CSR. **(A)** σ'_0 = 100 kPa, CSR = 0.25, σ_d = 50 kPa; **(B)** σ'_0 = 200 kPa, CSR = 0.25, σ_d = 100 kPa; **(C)** σ'_0 = 300 kPa, CSR = 0.25, σ_d = 150 kPa.

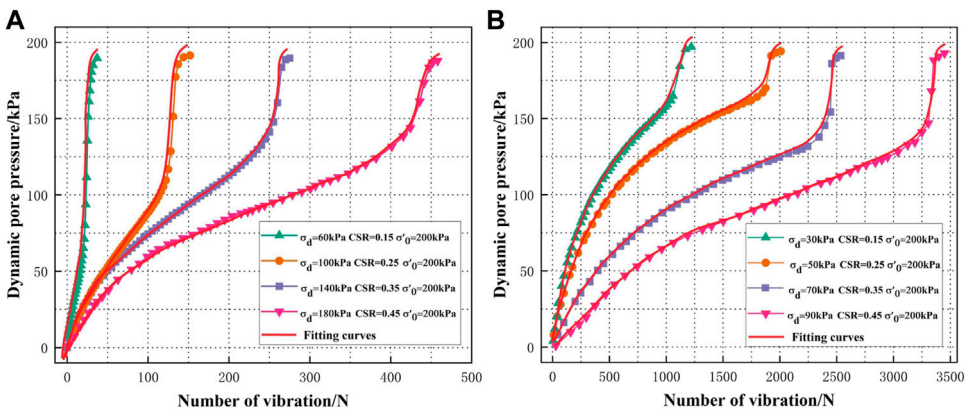

FIGURE 8 | Development curves of accumulated pore pressure of PG under different vibration conditions: **(A)** unidirectional vibrations condition; **(B)** bidirectional vibrations condition.

of PG under the same conditions, analyzes its development law of pore pressure, and discusses the dynamic stress-strain curve.

Figure 6 shows the development curves of the pore pressure of PG under the same conditions. The test results show that when the consolidation confining pressure is low (σ'_0 < 200 kPa), the liquefaction rate of PG gradually accelerates with the increase in consolidation confining pressure and dynamic stress, and the increase in consolidation confining pressure is the dominant factor of PG liquefaction; when the consolidation confining pressure is high (σ'_0 > 200 kPa), the liquefaction rate of PG gradually decreases with the increase in consolidation confining pressure and dynamic stress, and the increase in consolidation confining pressure is the dominant factor of PG liquefaction; when σ'_0 =

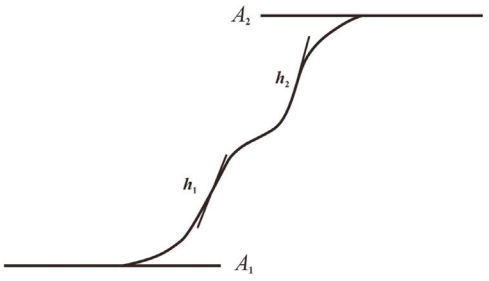

FIGURE 9 | BiDoseResp function characteristics.

200 kPa and σ_d = 100 k Pa, the liquefaction rate of PG is the fastest, and the cycle number is about 270 times.

When the confining pressure is low, with the rise of the confining pressure, some of the pore water and bound water in the PG skeleton seep out in a large amount (Shen et al., 2008), and some of the interparticle contact point lattices distort and deform, leading to smaller growth of the anti-liquefaction ability of PG with the increase in the confining pressure. Because PG has the property of being slightly soluble in water, some water channels form inside the specimens at the saturation stage (Zhang et al., 2007). At small amplitudes, some particles gradually move to the water channels. However, the water channels are not completely closed, and the particles gradually disorder and tend to be unstable under the vibration load. Therefore, at this stage, dynamic stress is the dominant factor of specimen liquefaction, and the dynamic strength gradually decreases with the growth of confining pressure and dynamic stress.

When the confining pressure is high, most of the pore water and bound water in PG have been discharged. With the increase in confining pressure, the interparticle connection tends to close, and PG stability gradually increases, so the increase in confining pressure enhances the anti-liquefaction ability of PG. At large amplitudes, most particles quickly move to and block the internal pores and water channels of PG to stabilize the sample structure. Therefore, at this stage, the consolidation confining pressure is the dominant factor of specimen liquefaction, and the dynamic strength gradually increases with the growth of confining pressure and dynamic stress.

When confining pressure is low, some of the pore water and bound water in the PG skeleton seep out in a large amount; near σ_0' = 200 kPa when the pore water and bound water began to drain completely; when σ_0' > 200 kPa, with the confining pressure continuing to increase, the particles gradually become dense and stabilized, so near σ_0' = 200 kPa when the PG reached the critical confining pressure. Similarly, near σ_d = 100 kPa, the water channels gradually closed, so near σ_d = 100 kPa PG reached the critical dynamic stress. Therefore, under the conditions of σ_0' = 200 kPa and σ_d = 100 kPa, there is a critical phenomenon of PG liquefaction rate, and the liquefaction rate reaches the fastest at this time.

If we continue to increase the consolidation confining pressure and dynamic stress (σ_0' = 600 kPa, σ_d = 300 kPa), the number of cycles required for liquefaction can reach 1,070 times, as shown in **Table 2**, indicating that the interparticle connection of PG tends to be tightened under high confining pressure, and the dynamic strength increases if we continue to increase the confining pressure and dynamic stress under the same CSR conditions.

3.2.2 The Analysis of Dynamic Stress–Strain Hysteresis Curves

Comparing the dynamic stress-strain curves of PG under different conditions in **Figure 7**, we can find that PG is axially compressed under cyclic loading. With the increase in the number of cycles, the centers of the curves keep moving in the direction of axial compression, producing plastic damage, and reflecting the deformation accumulation characteristics of PG to cyclic loading. Under cyclic loading, PG strain steadily increases after reaching the initial effective stress, showing cyclic activity. After the structural damage, the dynamic stress that the specimens can withstand decreases and converges to a constant value (**Figure 7C**). Before the structural damage of PG specimens, the axial strain hardly changes, indicating that the PG has high strength before the structural damage, but with the continuous application of cyclic loading, the PG structure is damaged, and the deformation increases rapidly.

TABLE 3 | Fitting results of model parameters.

Test number	A_1	A_2	c	v_1	v_2	h_1	h_2	R^2
1-1	−0.112	1.017	0.502	56.46	400.68	0.003	0.0008	0.997
1-2	−0.478	1.252	0.663	30.10	521.35	0.007	0.019	0.991
1-3	−0.478	1.304	0.541	40.25	271.22	0.011	0.022	0.992
1-4	−0.124	1.411	0.334	20.25	341.73	0.013	0.009	0.994
1-5	−0.307	1.043	0.737	58.14	420.54	0.015	0.076	0.996
2-1	−0.302	1.308	0.480	451.91	28.97	0.013	0.005	0.995
2-2	−0.220	1.301	0.541	40.65	271.24	0.047	0.055	0.993
2-3	−0.162	1.024	0.348	129.74	41.57	0.077	0.094	0.998
2-4	0.017	1.333	0.476	40.23	23.64	0.148	0.185	0.994
3-1	−1.208	1.457	0.679	365.64	350.35	0.0008	0.0005	0.990
3-2	−0.343	1.231	0.755	113.53	2005.13	0.0023	0.0034	0.992
3-3	−0.902	1.207	0.820	21.65	273.55	0.0044	0.0023	0.992
3-4	−0.546	1.206	0.748	10.13	1,133.64	0.0057	0.0062	0.995

FIGURE 10 | Softening phenomenon of PG after liquefaction by bidirectional vibrations.

Under the same CSR conditions, when the confining pressure is low (σ_0' < 200 kPa), the dynamic stress applied to the PG is small, and the pore pressure grows slowly to the consolidation confining pressure to complete liquefaction, at which time the peak value of the dynamic stress-strain hysteresis curve remains unchanged, and the specimens still have a large load-bearing capacity (**Figure 7A**). When the confining pressure is high (σ_0' > 200 kPa), with the increase in dynamic stress, the growth rate of pore pressure gradually accelerates, the structures of the specimens are damaged after liquefaction, and the cyclic loading-bearing capacity reduces (**Figure 7B**). At this time, the peak values of the dynamic stress-strain hysteresis curves decrease. In addition, the density of the hysteresis curves reflects the dynamic strength of the specimens to a certain extent. Under the same CSR conditions, the hysteresis curve when σ_0' = 100 kPa is denser than that when σ_0' = 200 kPa and σ_0' = 300 kPa, indicating that PG has higher strength when σ_0' = 100 kPa. This conclusion is verified in the aforementioned pore pressure law.

3.3 Comparison of Pore Pressure Development and Study of the Growth Model of PG Under Unidirectional and Bidirectional Vibrations With Different CSR Conditions

3.3.1 The Development Law of the Pore Pressure of PG With Unidirectional and Bidirectional Vibrations Under Different CSR Conditions

As shown in **Figure 8**, under the same consolidation confining pressure, the development laws of accumulated pore pressure under unidirectional and bidirectional vibrations are roughly the same. The liquefaction rate of PG gradually accelerates with the increase in CSR, and the number of vibrations required for liquefaction by bidirectional vibrations (**Figure 8B**) is much larger than that by unidirectional vibrations (**Figure 8A**). When CSR = 0.45, the specimens are cycled 36 times under unidirectional vibrations to complete liquefaction, while they are cycled more than 1,220 times under bidirectional vibrations to complete liquefaction.

3.3.2 BiDoseResp Pore Pressure Growth Model of PG

Previous scholars have proposed corresponding pore pressure growth models, such as the inverse sine trigonometric function model proposed by Seed et al. (1966) and the growth model of dynamic pore water pressure applicable to tailings materials proposed by Zhang et al. (2006) based on seed. However, the aforementioned pore pressure growth models can only describe the growth curves of dynamic pore pressure at stages in which a small amount of accumulated pore pressure grows, which are not applicable to the multi-stage accumulated dynamic pore pressure of PG. Combining the test results and the curve characteristics at each stage and citing the BiDoseResp function of the dynamic pore pressure growth model (Du et al., 2016) of tailings silt (as shown in **Figure 9** and **Eq. 2**), we found that the characteristics at each stage of PG pore pressure growth were consistent with the h_1-A_2 section curve in the BiDoseResp function:

$$y = A_1 + (A_2 - A_1) \times \left[\frac{c}{1 + 10^{(v_1 - x)h_1}} + \frac{1 - c}{1 + 10^{(v_2 - x)h_2}} \right] \quad (2)$$

where A_1, A_2, c, v_1, v_2, h_1, and h_2 are model parameters; A_1 and A_2 are the range of the model; h_1 is the slope of the pore pressure curve at the rapid growth stage; and h_2 is the slope of the curve at the instantaneous failure stage. The fitted curves are shown in **Figures 6** and **8**. The BiDoseResp function is used to fit the curves of PG pore pressure ratio versus vibrations under unidirectional and bidirectional vibrations, and the fitting effect is good. The specific fitting parameters are shown in **Table 3**. The fitting results in **Table 3** indicate that the slopes of the curves at the rapid growth stage and the instantaneous failure stage under unidirectional and bidirectional vibrations increase with the increase in CSR, and the growth rates of pore pressure at the rapid growth stage and the instantaneous failure stage under unidirectional vibrations are greater than those under bidirectional vibrations. In addition, the fluctuation range of parameters v_1 and v_2 is large, and the fluctuation range of the remaining parameters is relatively small. The fitting degree is more than 0.990. Therefore, it can be considered that the model has good applicability to the development law of the accumulated pore pressure of saturated PG under unidirectional and bidirectional vibrations.

3.4 Softening Phenomenon of PG Under Bidirectional Vibrations

While the pore water pressure rises under cyclic loading, the strength of PG softens. To ensure the safety and stability of PG dams under seismic action, it is important to study the strength softening law of PG under cyclic loading. By conducting

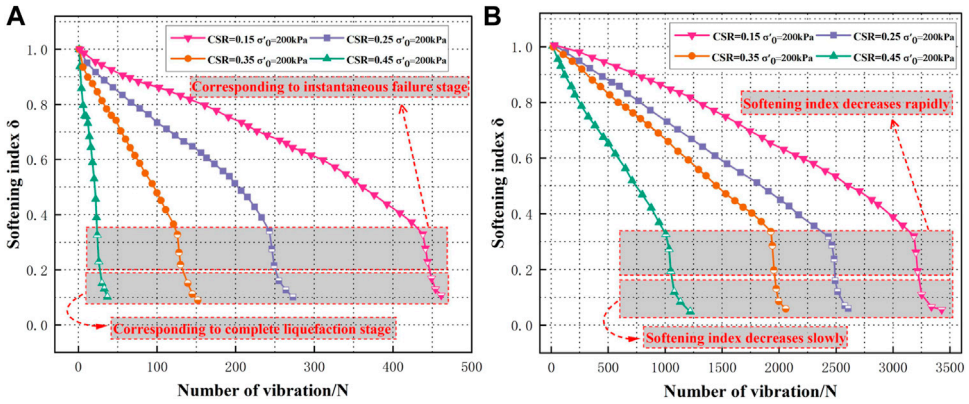

FIGURE 11 | Effect of different CSR on softening index of PG under different vibration condition: **(A)** unidirectional vibrations condition; **(B)** bidirectional vibrations condition.

unidirectional and bidirectional vibration tests on PG under the same CSR conditions, we found that PG had a significant strain-softening phenomenon after liquefaction by bidirectional vibration (**Figure 10**). Numerous scholars have studied the cyclic softening of soil: Idriss et al. (1978) firstly proposed the softening index. Considering the effect of initial consolidation confining pressure, Wang et al. (2009) redefined the softening index δ as (**Eq. 3**):

$$\delta = \frac{G_N}{G_1} = \frac{\frac{q_{max}-q_{min}}{\varepsilon_{N,max}-\varepsilon_{N,min}}}{\frac{q_{max}-q_{min}}{\varepsilon_{1,max}-\varepsilon_{1,min}}} = \frac{\frac{2\sigma_d}{\varepsilon_{N,max}-\varepsilon_{N,min}}}{\frac{2\sigma_d}{\varepsilon_{1,max}-\varepsilon_{1,min}}} = \frac{\varepsilon_{1,max}-\varepsilon_{1,min}}{\varepsilon_{N,max}-\varepsilon_{N,min}} \quad (3)$$

where q_{max} and q_{min} are the maximum and minimum deviatoric stress of the soil sample in each cycle; $\varepsilon_{1,max}$ and $\varepsilon_{1,min}$ are the maximum and minimum axial strains in the first cycle; and $\varepsilon_{N,max}$ and $\varepsilon_{N,min}$ are the maximum and minimum axial strains in the *N*th cycle, respectively.

From the development curves of the softening index δ in **Figure 11**, it can be observed that:

1) With the increase in cyclic vibration times, the softening indexes of PG under unidirectional and bidirectional vibrations are gradually reduced. Under the same consolidation confining pressure, larger CSR suggests a faster decrease in the softening index and a higher softening degree. The softening index curves of PG under unidirectional and bidirectional vibrations have the same decreasing trends. When the softening index decreases to about 0.3 at the later liquefaction stage, the softening index of PG decreases rapidly under both unidirectional and bidirectional vibrations, and the softening of PG is accelerated, corresponding to the instantaneous failure stage. When the softening index decreases to about 0.2, the softening index decreases slowly to the minimum, corresponding to the complete liquefaction stage. The decreasing rate of PG softening indexes during liquefaction is positively correlated with the growth rate of pore pressure, indicating that the strength softening of PG is mainly caused by the growth of dynamic pore pressure, which leads to the structural damage of the specimens.
2) Under the same CSR conditions, the number of vibrations required for liquefaction of PG by bidirectional vibrations is significantly higher than that by unidirectional vibrations, but the softening index of liquefaction by bidirectional vibrations is slightly lower than that by unidirectional vibrations, indicating that the structural damage of PG is more adequate under bidirectional vibrations, the integrity of the specimens is significantly reduced after liquefaction, and PG has significant strain-softening characteristics and presents certain mobility.

4 CONCLUSION

In this article, through the dynamic triaxial tests of PG under different consolidation and vibration conditions. The main conclusions are as follows:

1) The development curve of instantaneous pore pressure of PG under unidirectional vibrations can be divided into the rapid growth stage of pore pressure, the stable growth stage of pore pressure, the instantaneous failure stage, and the complete liquefaction stage. Under bidirectional vibrations, it can be divided into the rapid growth stage of pore pressure, the stable growth stage of pore pressure, the slow growth stage of pore pressure, the instantaneous failure stage, and the complete liquefaction stage.
2) The joint effect of consolidation confining pressure and dynamic stress on PG was explored. Due to the special consolidation and physical properties of PG, the liquefaction strength does not increase monotonically with the increase in dynamic stress and consolidation confining pressure under unidirectional vibrations with CSR = 0.25. However, there is a critical point when σ_0' = 200 kPa and σ_d = 100 kPa, and under this condition, the liquefaction rate of PG reaches the highest.
3) The comparison tests of unidirectional and bidirectional vibrations of PG under the same CSR conditions show that the number of vibrations required for liquefaction of PG under bidirectional vibrations is much larger than that under unidirectional vibrations, the increasing trends of accumulated pore pressure are roughly the same, and the

development curves of accumulated pore pressure under both the vibrations can be fitted by BiDoseResp function model with good consistency.

4) After liquefaction by bidirectional vibrations, the structure of PG is completely destroyed, and PG is significantly softened and presents certain flow characteristics. The research results have certain reference significance for the seismic design of PG dams.

DATA AVAILABILITY STATEMENT

The original contributions presented in the study are included in the article/Supplementary Material, further inquiries can be directed to the corresponding author.

AUTHOR CONTRIBUTIONS

Conceptualization: FK, GW, and WL; methodology: FK, and GW; formal analysis and investigation: FK, XL, and WZ; validation: FK and ZD; writing—review and editing: FK, GW, WL, and MW.

FUNDING

The research work was funded by the National Natural Science Foundation of China (No. 52174114), and the open fund project of the National Engineering and Technology Research Center for Development & Utilization of Phosphate Resources(No. NECP2022-07).

REFERENCES

Cao, Y., Cui, Y., Yu, X., Li, T., Chang, I.-S., and Wu, J. (2021). Bibliometric Analysis of Phosphogypsum Research from 1990 to 2020 Based on Literatures and Patents. *Environ. Sci. Pollut. Res.* 28 (47), 66845–66857. doi:10.1007/s11356-021-15237-y

Du, Y. Q., Yang, C. H., and Wu, S. W. (2016). Pore-Water Pressure Characteristics of Tailings Silt under Cyclic Loading. *J. Northeast. Univ. Nat. Sci.* 37 (04), 583–588. doi:10.3969/j.issn.1005-3026.2016.04.027

Global (2018). *State Administration for Market Regulation of the People's Republic of China*. Beijing: Phosphogypsum. (GB 23456-2018) (in Chinese).

Idriss, I. M., Dobry, R., and Singh, R. D. (1978). Nonlinear Behavior of Soft Clays during Cyclic Loading. *J. Geotech. Engrg. Div.* 104 (12), 1427–1447. doi:10.1061/AJGEB6.0000727

Liu, J. X., Zhang, J. X., Yuan, H. C., Wang, G. J., Fan, X. Y., and Li, X. N. (2021). Investigation on the Dynamic Characteristics in Unidirectional and Bidirectional Vibration of Saturated Tail Sand under High Stress Conditions. *Earthq. Eng. Eng.* 41 (06), 1–10. doi:10.13197/j.eeev.2021.06.1.liujx.001

Lu, T., Wang, W., Wei, Z., Yang, Y., and Cao, G. (2021). Experimental Study on Static and Dynamic Mechanical Properties of Phosphogypsum. *Environ. Sci. Pollut. Res.* 28 (14), 17468–17481. doi:10.1007/s11356-020-12148-2

Mi, Z. K., Rao, X. S., Chu, X. Q., and Cao, P. (2015). Physico-mechanical Properties of Deposition Phosphogypsum. *Chin. J. Geotechnical Eng.* 37 (03), 470–478. doi:10.11779/CJGE201503010

People's Republic of China (2016). *Safety Technical Regulation on Phosphogypsum Stack*. Beijing: State Administration of Work Safety. AQ 2059-2016) (in Chinese).

Rascol, E., and Lausanne, D]. (2009). *Cyclic Properties of Sand: Dynamic Behaviour for Seismic Applications*. Switzerland: EPFL.

Rico, M., Benito, G., Salgueiro, A. R., Díez-Herrero, A., and Pereira, H. G. (2008). Reported Tailings Dam Failures: A Review of the European Incidents in the Worldwide Context. *J. Hazard. Mater.* 152 (2), 846–852. doi:10.1016/j.jhazmat.2007.07.050

Seed, H. B., and Idriss, I. M. (1971). Simplified Procedure for Evaluating Soil Liquefaction Potential. *J. Soil Mech. Found. Div.* 97 (9), 1249–1273. doi:10.1061/jsfeaq.0001662

Seed, H. B., and Lee, K. L. (1966). Liquefaction of Saturated Sands during Cyclic Loading. *J. Soil Mech. Found. Div.* 92 (6), 105–134. doi:10.1061/jsfeaq.0000913

Shen, T., Wang, W., and Li, G. Y. (2008). The Physical Mechanical Properties of Phosphogypsum. *Phosphate Compd. Fertilizer* 23 (03), 21–23. doi:10.3969/j.issn.1007-6220.2008.03.006

Tayibi, H., Choura, M., López, F. A., Alguacil, F. J., and López-Delgado, A. (2009). Environmental Impact and Management of Phosphogypsum. *J. Environ. Manag.* 90 (8), 2377–2386. doi:10.1016/j.jenvman.2009.03.007

Wang, J., Cai, Y. Q., and Pan, L. Y. (2009). Degradation of Stiffness of Soft Clay under Bidirectional Cyclic Loading. *Chin. J. Geotechnical Eng.* 31 (02), 934–944. doi:10.3321/j.issn:1000-4548.2009.02.005

Wang, M., Kong, L., Zhao, C., and Zang, M. (2012). Dynamic Characteristics of Lime-Treated Expansive Soil under Cyclic Loading. *J. Rock Mech. Geotechnical Eng.* 4 (4), 352–359. doi:10.3724/SP.J.1235.2012.00352

Wang, G., Tian, S., Hu, B., Chen, J., and Kong, X. (2021). Regional Hazard Degree Evaluation and Prediction for Disaster Induced by Discharged Tailings Flow from Dam Failure. *Geotech. Geol. Eng.* 39 (2), 2051–2063. doi:10.1007/s10706-020-01606-w

Xie, Q. F., and Liu, G. B. (2017). An Experimental Study of the Strength Weakening Characteristic of Clay under Two Different Vibration Modes. *Hydrogeology Eng. Geol.* 44 (5), 66–71+79. doi:10.16030/j.cnki.issn.1000-3665.2017.05.11

Xie, D. Y. (2011). *Soil Dynamics*. Bei Jing: Higher Education Press.

Xu, X. Y., Xu, Y. Z., Chen, G. S., and Yu, X. J. (2008). Testing Study on Engineering Chearacteristics of Phosphogypsum. *Chin. J. Rock Mech. Eng.* 37 (03), 470–478. doi:10.11779/CJGE201503010

You, W., Dai, F., Liu, Y., Du, H., and Jiang, R. (2021). Investigation of the Influence of Intermediate Principal Stress on the Dynamic Responses of Rocks Subjected to True Triaxial Stress State. *Int. J. Min. Sci. Technol.* 31 (5), 913–926. doi:10.1016/j.ijmst.2021.06.003

Zhang, C., Yang, C. H., and Bai, S. W. (2006). Experimental Study on Dynamic Characteristics of Tailings Material. *Rock Soil Mech.* 27 (01), 35–40. doi:10.16285/j.rsm.2006.01.007

Zhang, C., Yang, C. H., Yu, K. J., Fu, S. W., and Chen, F. (2007). Study on Physico-Mechanical Characteristics of Phosphogypsum. *Rock Soil Mech.* 28 (03), 461–466. doi:10.16285/j.rsm.2007.03.006

Zhang, X. Z., Wu, S. W., Zhang, C., and Yang, C. H. (2018). Dynamic Pore-Water Pressure Evolution of Tailings Under Different Consolidation Conditions. *Rock Soil Mech.* 39 (03), 815–822. doi:10.16285/j.rsm.2016.0921

Zhang, L. Z., Zhang, Y. X., Zhang, X. F., Tan, X. M., and Lv, Z. H. (2019). Research Progress on Resource Utilization of Phosphogypsum in China. *Conservation Util. Mineral Resour.* 39 (04), 14–18. doi:10.13779/j.cnki.issn1001-0076.2019.04.003

Zheng, Y., Chen, C., Wang, R., and Meng, F. (2022). Stability Analysis of Rock Slopes Subjected to Block-Flexure Toppling Failure Using Adaptive Moment Estimation Method (Adam). *Rock Mech. Rock Eng.* 55, 3675–3686 doi:10.1007/s00603-022-02828-5

Zhou, Y., Sheng, Q., Li, N., and Fu, X. (2022). The Dynamic Mechanical Properties of a Hard Rock under True Triaxial Damage-Controlled Dynamic Cyclic Loading with Different Loading Rates: a Case Study. *Rock Mech. Rock Eng.* 55 (4), 2471–2492. doi:10.1007/s00603-021-02756-w

Conflict of Interest: Author WL is employed by China nonferrous metals industry Kunming survey and design research institute Co.LTD. Author MW is employed by National Engineering Research Center for Development and Utilization of Phosphorus Resources, Yunnan phosphate group Co. LTD.

The remaining authors declare that the research was conducted in the absence of any commercial or financial relationships that could be construed as a potential conflict of interest.

Publisher's Note: All claims expressed in this article are solely those of the authors and do not necessarily represent those of their affiliated organizations, or those of the publisher, the editors, and the reviewers. Any product that may be evaluated in this article, or claim that may be made by its manufacturer, is not guaranteed or endorsed by the publisher.